

# Polarimetric imprints of exotic compact objects

Hanna Liis Tamm  
João Luís Rosa, Nicolas Aimar

July 2, 2026

## ① **Motivation**

② Overview of models

③ Polarization and setup

④ Simulation results

⑤ Conclusions

# Detection of infra-red flares [1]- [3]

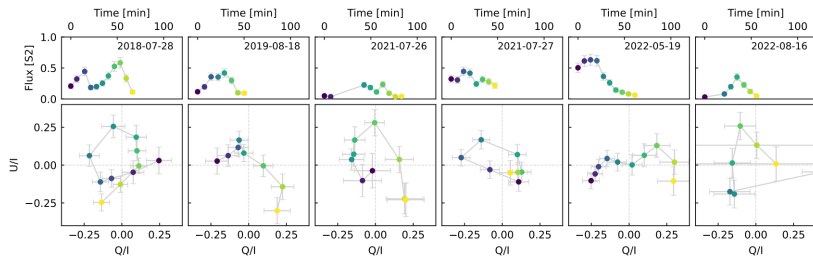


Figure: The flux evolution (top row) and polarimetric signatures  $Q/I$ ,  $U/I$  (bottom row) of flares measured by GRAVITY. [3]

# Detection of infra-red flares [1]- [3]

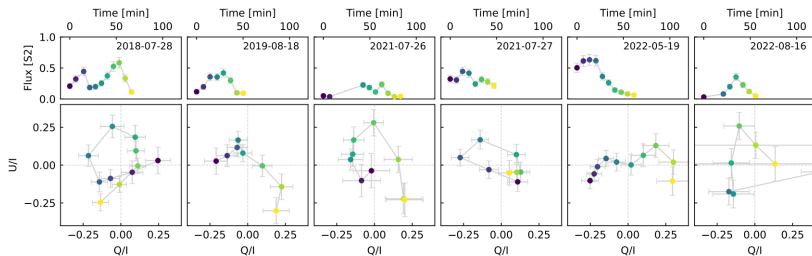
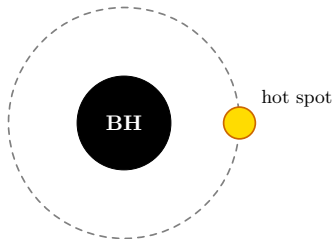


Figure: The flux evolution (top row) and polarimetric signatures  $Q/I$ ,  $U/I$  (bottom row) of flares measured by GRAVITY. [3]

Implications on...



# Detection of infra-red flares [1]- [3]

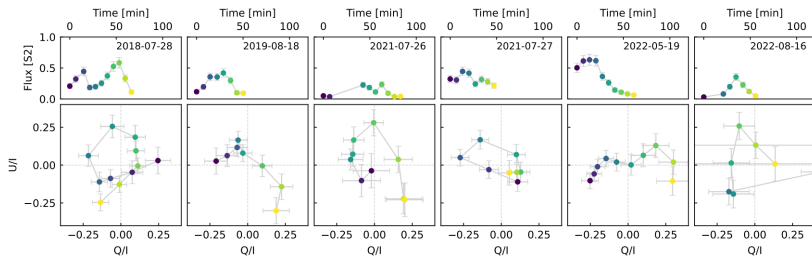
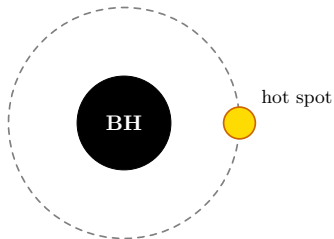


Figure: The flux evolution (top row) and polarimetric signatures  $Q/I$ ,  $U/I$  (bottom row) of flares measured by GRAVITY. [3]

Implications on...



- BH spin

# Detection of infra-red flares [1]- [3]

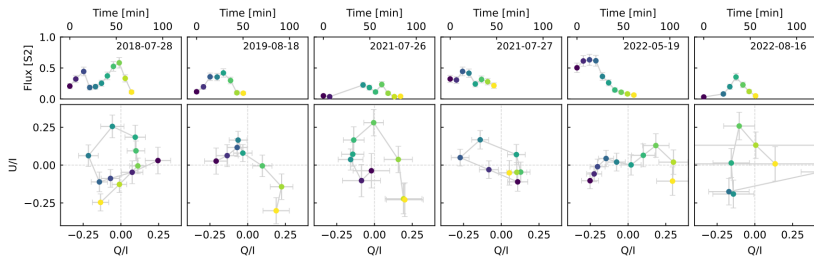
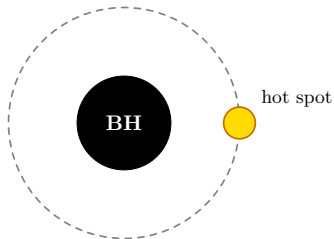


Figure: The flux evolution (top row) and polarimetric signatures  $Q/I$ ,  $U/I$  (bottom row) of flares measured by GRAVITY. [3]

Implications on...

- BH spin
- magnetic field structure



# Detection of infra-red flares [1]- [3]

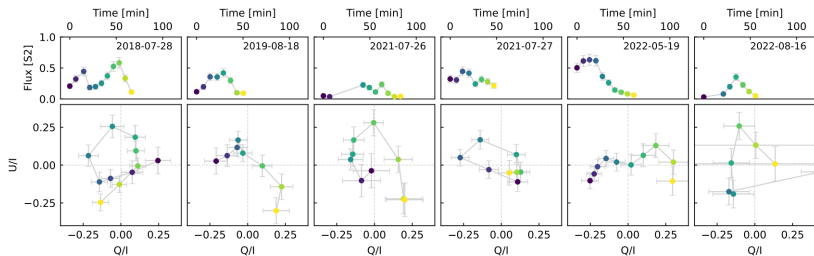
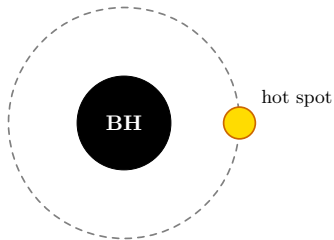


Figure: The flux evolution (top row) and polarimetric signatures  $Q/I$ ,  $U/I$  (bottom row) of flares measured by GRAVITY. [3]



Implications on...

- BH spin
- magnetic field structure
- hot-spot properties

# Detection of infra-red flares [1]- [3]

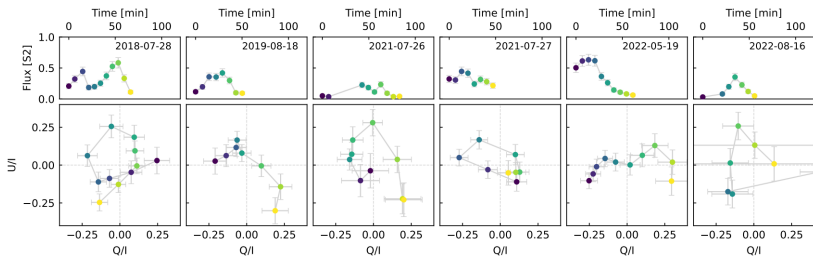
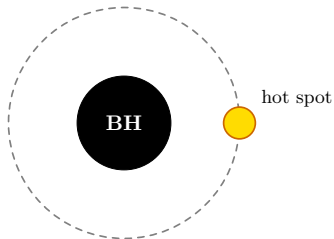


Figure: The flux evolution (top row) and polarimetric signatures  $Q/I$ ,  $U/I$  (bottom row) of flares measured by GRAVITY. [3]



Implications on...

- BH spin
- magnetic field structure
- hot-spot properties
- **geometry**

# Motivation

- GR is successful, but incomplete
- Fundamental questions: cosmic censorship conjecture, information loss

# Motivation

- GR is successful, but incomplete
- Fundamental questions: cosmic censorship conjecture, information loss
- Black-hole mass gap  $\rightarrow$  exotic matter, new formation channels

# Motivation

- GR is successful, but incomplete
- Fundamental questions: cosmic censorship conjecture, information loss
- Black-hole mass gap  $\rightarrow$  exotic matter, new formation channels
- Alternatives to BHs – exotic compact objects (ECOs)
  - Examine the effects of matter structure, compacticity, anomalies

# Motivation

- GR is successful, but incomplete
- Fundamental questions: cosmic censorship conjecture, information loss
- Black-hole mass gap  $\rightarrow$  exotic matter, new formation channels
- Alternatives to BHs – exotic compact objects (ECOs)
  - Examine the effects of matter structure, compacticity, anomalies
- We will consider:
  - relativistic fluid spheres (FS)
  - gravitational vacuum stars (GS)
  - solitonic boson stars (SBS)

- ① Motivation
- ② **Overview of models**
- ③ Polarization and setup
- ④ Simulation results
- ⑤ Conclusions

# Theory of ECOs: FS

- Interior fluid (dark matter), exterior vacuum

$$g_{tti} = -\frac{1}{4} \left( 3\sqrt{1 - \frac{2M}{R}} - \sqrt{1 - \frac{2r^2M}{R^3}} \right)^2 \quad g_{tte} = - \left( 1 - \frac{2M}{r} \right) \quad (1)$$

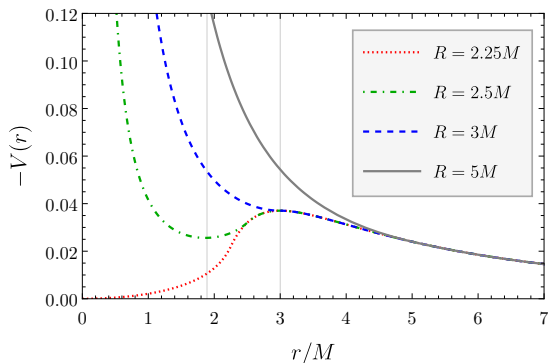
$$g_{rri} = \left( 1 - \frac{2r^2M}{R^3} \right)^{-1} \quad g_{rre} = \left( 1 - \frac{2M}{r} \right)^{-1} \quad (2)$$

# Theory of ECOs: FS

- Interior fluid (dark matter), exterior vacuum

$$g_{tti} = -\frac{1}{4} \left( 3\sqrt{1 - \frac{2M}{R}} - \sqrt{1 - \frac{2r^2M}{R^3}} \right)^2 \quad g_{tte} = - \left( 1 - \frac{2M}{r} \right) \quad (1)$$

$$g_{rri} = \left( 1 - \frac{2r^2M}{R^3} \right)^{-1} \quad g_{rre} = \left( 1 - \frac{2M}{r} \right)^{-1} \quad (2)$$



Potential for FS models.  
Extrema depict the existence  
and type of LR. [4]

# Theory of ECOs: GS

- Interior fluid (dark energy), exterior vacuum

$$g_{tti} = -\alpha \left(1 - \frac{2m(r)}{r}\right) \quad g_{tte} = - \left(1 - \frac{2M}{r}\right) \quad (3)$$

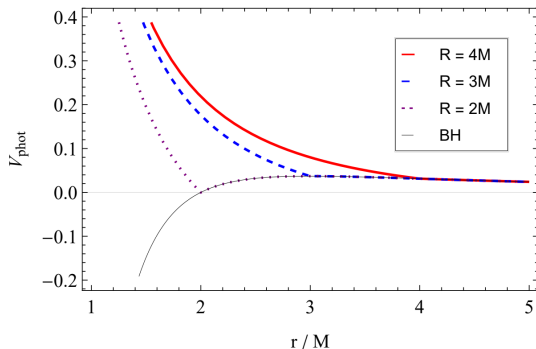
$$g_{rri} = \alpha^{-1} \left(1 - \frac{2m(r)}{r}\right)^{-1} \quad g_{rre} = \left(1 - \frac{2M}{r}\right)^{-1} \quad (4)$$

# Theory of ECOs: GS

- Interior fluid (dark energy), exterior vacuum

$$g_{tti} = -\alpha \left(1 - \frac{2m(r)}{r}\right) \quad g_{tte} = - \left(1 - \frac{2M}{r}\right) \quad (3)$$

$$g_{rri} = \alpha^{-1} \left(1 - \frac{2m(r)}{r}\right)^{-1} \quad g_{rre} = \left(1 - \frac{2M}{r}\right)^{-1} \quad (4)$$



Potential for GS models.  
Extrema depict the existence  
and type of LRs. [6]

# Theory of ECOs: SBS [7]

- Interior scalar field, asymptotically vacuum

$$S = \int_{\Omega} \sqrt{-g} \left[ \frac{R}{16\pi} - \frac{1}{2} \partial_{\mu} \Phi^* \partial^{\mu} \Phi - \frac{1}{2} V(|\Phi|^2) \right] d^4x, \quad (5)$$

$$V(|\Phi|^2) = \mu^2 |\Phi|^2 \left( 1 + \frac{|\Phi|^2}{\alpha^2} \right)^2 \quad (6)$$

# Theory of ECOs: SBS [7]

- Interior scalar field, asymptotically vacuum

$$S = \int_{\Omega} \sqrt{-g} \left[ \frac{R}{16\pi} - \frac{1}{2} \partial_{\mu} \Phi^* \partial^{\mu} \Phi - \frac{1}{2} V(|\Phi|^2) \right] d^4x, \quad (5)$$

$$V(|\Phi|^2) = \mu^2 |\Phi|^2 \left( 1 + \frac{|\Phi|^2}{\alpha^2} \right)^2 \quad (6)$$

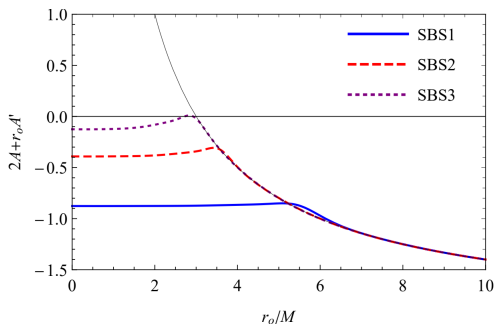


Figure: The expression  $2A(r_0) - r_0 A'(r_0)$  for discriminating LRs for three BS models. The zeroes of the expression correspond to LR orbits. [7]

- ① Motivation
- ② Overview of models
- ③ **Polarization and setup**
- ④ Simulation results
- ⑤ Conclusions

# Polarization parameters

- Stokes parameters, EVPA,  $QU$ -loops

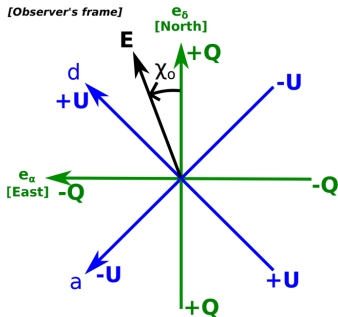
$$I = E^2 \quad (7)$$

$$Q = I \cos(2\chi_0) \quad (8)$$

$$U = I \sin(2\chi_0) \quad (9)$$

$$\chi_0 = \text{atan2}(Q, U) \quad (10)$$

- Magnetic field configuration: vertical/poloidal



Electric field, EVPA and Stokes  $Q$  and  $U$  defined in the observer's frame. [8]

# Simulations in GYOTO

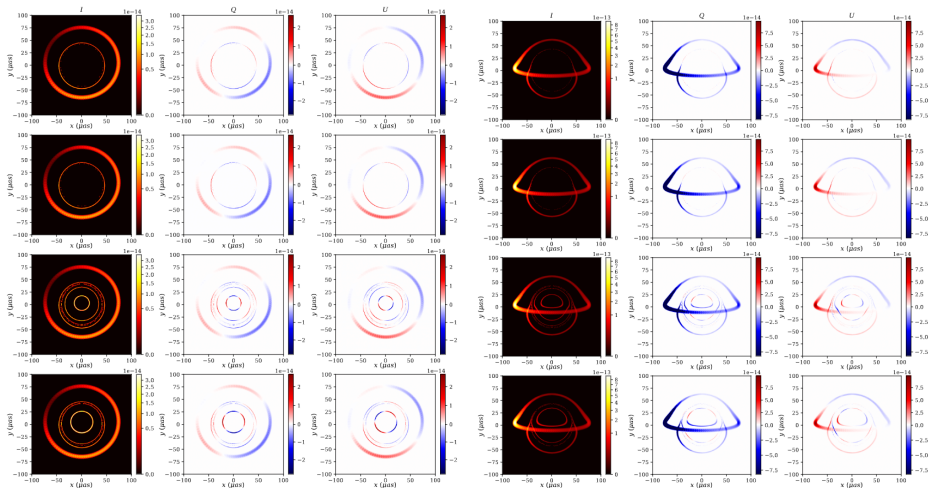
- $r_o = 8M, i \in \{20^\circ, 80^\circ\}$

Model	$R/M$	# of LR(s)
SBH	-	1
FS1	2.25	1
FS2	2.50	2
FS3	3.00	2 (degen.)
GS1	3.00	2 (degen.)
GS2	2.50	2
GS3	2.01	2
SBS1	6.58	0
SBS2	3.95	0
SBS3	3.12	1

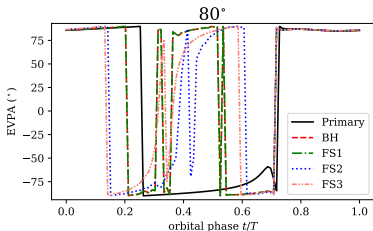
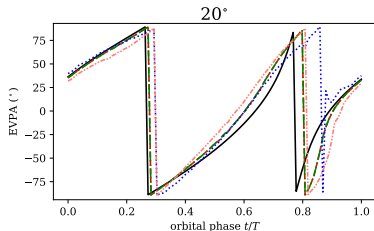
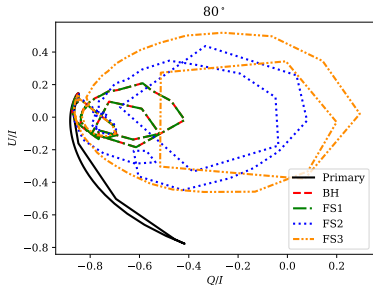
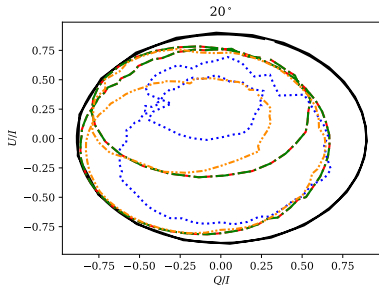
Property	Value
Compact object mass	$4.2 \cdot 10^{-6} M_\odot$
Compact object distance	8.25 kpc
Observing frequency	230 GHz
Screen resolution	1000 px
Screen field of view	$250 \mu\text{as}$
Inclination	$20^\circ, 80^\circ$
Time steps	100/200
Hot-spot radius	$0.5 M$
Hot-spot orbital radius	$8M$
Hot-spot temperature	200
Hot-spot number density	$6.6 \cdot 10^6 \text{ cm}^{-3}$
Magnetization parameter	0.01

- ① Motivation
- ② Overview of models
- ③ Polarization and setup
- ④ **Simulation results**
- ⑤ Conclusions

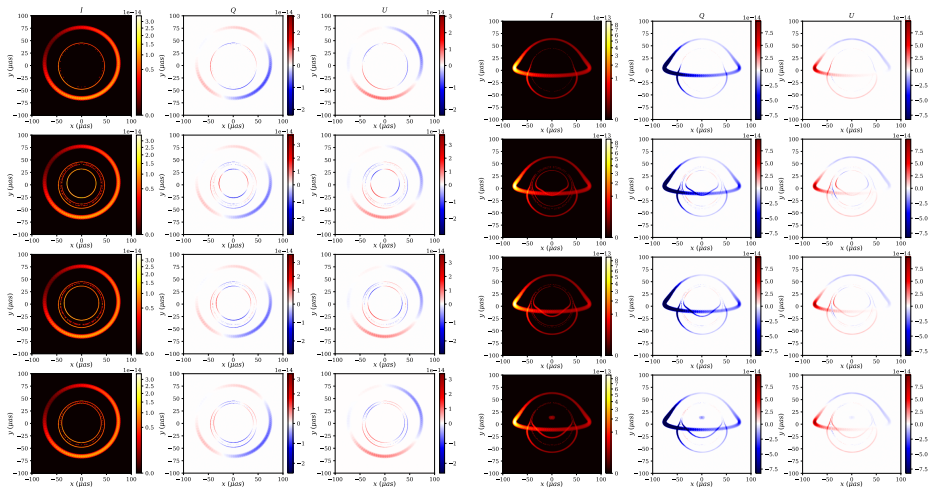
# Results: integrated images (FS)



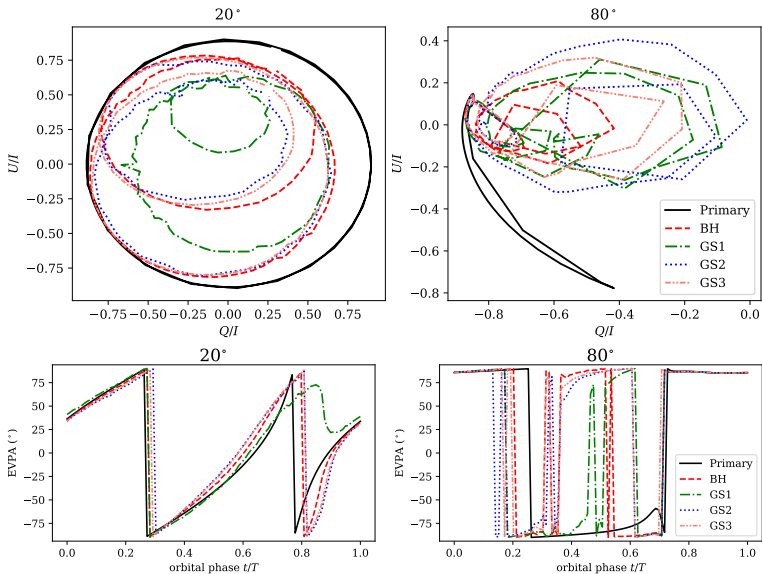
# Results: $QU$ -loops, EVPA (FS)



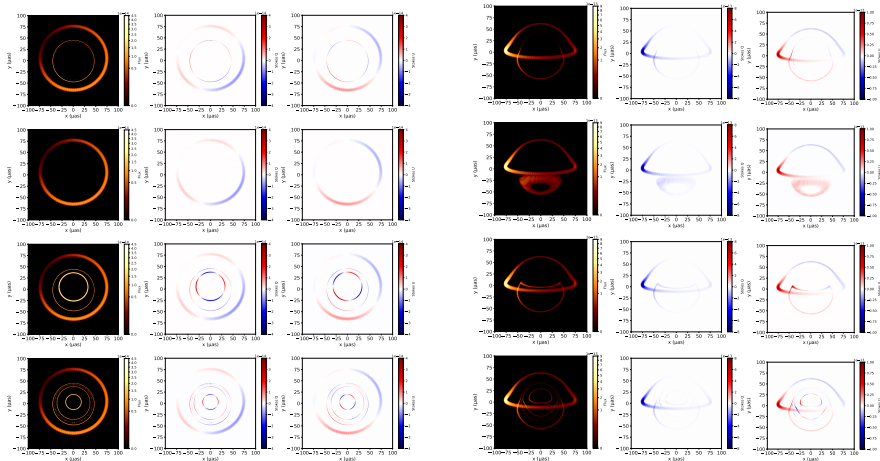
# Results: integrated images (GS)



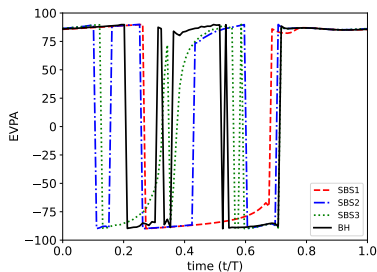
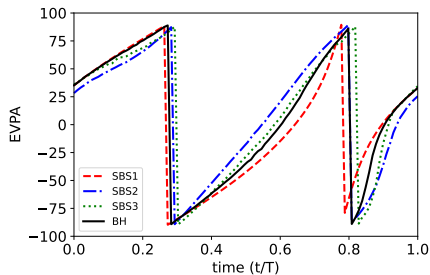
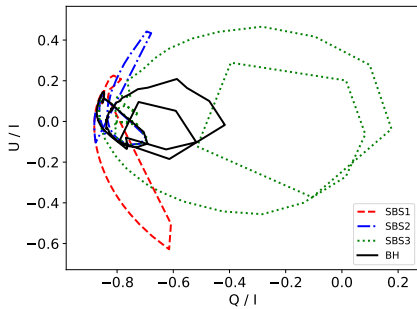
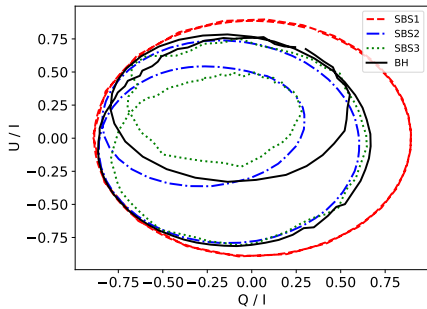
# Results: $QU$ -loops, EVPA (GS)



# Results: integrated images (SBS)



# Results: $QU$ -loops, EVPA (SBS)



## Quantitative comparison

Model	OLA	ILA	LAR	ST ( $T$ )
Primary	2.49	2.49	1.00	0.51
BH	1.88	1.17	0.62	0.53
FS1	1.88	1.17	0.62	0.53
FS2	1.35	0.27	0.20	0.57
FS3	1.83	0.67	0.36	0.52
GS1	1.22	0.24	0.19	0.60
GS2	1.79	0.73	0.41	0.52
GS3	1.83	0.89	0.48	0.53
SBS1	2.49	2.49	1.00	0.51
SBS2	1.78	0.79	0.44	0.51
SBS3	1.92	0.57	0.29	0.52

Table: Outer loop area (OLA), inner loop area (ILA), loop area ratio (LAR), and shift time (ST) as a fraction of the orbital period  $T$ , for the simulations with an observation angle of  $i = 20^\circ$ .

- ① Motivation
- ② Overview of models
- ③ Polarization and setup
- ④ Simulation results
- ⑤ **Conclusions**

# Conclusions

- Polarimetry allows for the distinction between models

# Conclusions

- Polarimetry allows for the distinction between models
- Matter content: one model **FS1** identical to BH (pressure singularity)

# Conclusions

- Polarimetry allows for the distinction between models
- Matter content: one model **FS1** identical to BH (pressure singularity)
- Compacticity: can eliminate one model **SBS1** due to the absence of higher order images

# Conclusions

- Polarimetry allows for the distinction between models
- Matter content: one model **FS1** identical to BH (pressure singularity)
- Compacticity: can eliminate one model **SBS1** due to the absence of higher order images
- Future detectability and extensions

# References

- [1] C. Goddi *et al.*, The Astrophysical Journal Letters **910** (2021), L14, doi:10.3847/2041-8213/abee6a [arXiv:2105.02272 [astro-ph.GA]]
- [2] K. Akiyama *et al.* [EHT], The Astrophysical Journal Letters **910** (2021), L12, doi:10.3847/2041-8213/abe71d [arXiv:2105.01169 [astro-ph.HE]]
- [3] R. Abuter *et al.* [GRAVITY], Astron. Astrophys. **677** (2023), L10, doi:10.1051/0004-6361/202347416 [arXiv:2307.11821 [astro-ph.GA]].
- [4] H. L. Tamm and J. L. Rosa, Physical Review D **109** (2024), 044062, doi:10.1103/PhysRevD.109.044062
- [5] J. L. Rosa, P. Piçarra, Physical Review D **102** (2020), 6, doi=10.1103/physrevd.102.064009 [arXiv:2006.09854 [gr-qc]]
- [6] J. L. Rosa *et al.*, Physical Review D **109** (2024), 8, doi=10.1103/physrevd.109.084002 [arXiv:2401.07766 [gr-qc]]
- [7] J. L. Rosa *et al.*, Physical Review D **108** (2023), 4, doi=10.1103/PhysRevD.108.04402
- [8] F. H. Vincent *et al.*, Astronomy & Astrophysics **684** (2024), A194, doi=10.1051/0004-6361/202348016 [arXiv:2309.10053 [astro-ph.HE]]

# Appendix

Fluid spheres:

$$g_{tti} = -\frac{1}{4} \left( 3\sqrt{1 - \frac{2M}{R}} - \sqrt{1 - \frac{2r^2M}{R^3}} \right)^2 \quad g_{tte} = - \left( 1 - \frac{2M}{r} \right) \quad (11)$$

$$g_{rri} = \left( 1 - \frac{2r^2M}{R^3} \right)^{-1} \quad g_{rre} = \left( 1 - \frac{2M}{r} \right)^{-1} \quad (12)$$

Gravastars:

$$g_{tti} = -\alpha \left( 1 - \frac{2m(r)}{r} \right) \quad g_{tte} = - \left( 1 - \frac{2M}{r} \right) \quad (13)$$

$$g_{rri} = \alpha^{-1} \left( 1 - \frac{2m(r)}{r} \right)^{-1} \quad g_{rre} = \left( 1 - \frac{2M}{r} \right)^{-1} \quad (14)$$

Solitonic boson stars:

$$ds^2 = -A(r)dt^2 + \frac{1}{B(r)}dr^2 + r^2d\Omega^2 \quad (15)$$

$$\Phi = \phi(r) e^{-i\omega t} \quad (16)$$

